Search at the Mainz Microtron for Light Massive Gauge Bosons Relevant for the Muon $g-2$ Anomaly

H. Merkel,[1,*] P. Achenbach,[1] C. Ayerbe Gayoso,[1,†] T. Beranek,[1] J. Beričič,[2] J. C. Bernauer,[1,‡] R. Böhm,[1] D. Bosnar,[3] L. Correa,[1] L. Debenjak,[2] A. Denig,[1] M. O. Distler,[1] A. Esser,[1] H. Fonvieille,[4] I. Friščić,[3] M. Gómez Rodríguez de la Paz,[1] M. Hoek,[1] S. Kegel,[1] Y. Kohl,[1] D. G. Middleton,[1] M. Mihovilovič,[1] U. Müller,[1] L. Nungesser,[1] J. Pochodzalla,[1] M. Rohrbeck,[1] G. Ron,[5] S. Sánchez Majos,[1] B. S. Schlimme,[1] M. Schoth,[1] F. Schulz,[1] C. Sfienti,[1] S. Širca,[2,6] M. Thiel,[1] A. Tyukin,[1] A. Weber,[1] and M. Weinriefer[1]
(A1 Collaboration)

[1]*Institut für Kernphysik, Johannes Gutenberg-Universität Mainz, D-55099 Mainz, Germany*
[2]*Jožef Stefan Institute, SI-1000 Ljubljana, Slovenia*
[3]*Department of Physics, University of Zagreb, HR-10002 Zagreb, Croatia*
[4]*Clermont Université, Université Blaise Pascal, CNRS/IN2P3, LPC, BP 10448, F-63000 Clermont-Ferrand, France*
[5]*Racah Institute of Physics, Hebrew University of Jerusalem, Jerusalem 91904, Israel*
[6]*Department of Physics, University of Ljubljana, SI-1000 Ljubljana, Slovenia*

(Received 22 April 2014; revised manuscript received 19 May 2014; published 4 June 2014)

A massive, but light, Abelian $U(1)$ gauge boson is a well-motivated possible signature of physics beyond the standard model of particle physics. In this Letter, the search for the signal of such a $U(1)$ gauge boson in electron-positron pair production at the spectrometer setup of the A1 Collaboration at the Mainz Microtron is described. Exclusion limits in the mass range of 40 MeV/c^2 to 300 MeV/c^2, with a sensitivity in the squared mixing parameter of as little as $\epsilon^2 = 8 \times 10^{-7}$ are presented. A large fraction of the parameter space has been excluded where the discrepancy of the measured anomalous magnetic moment of the muon with theory might be explained by an additional $U(1)$ gauge boson.

DOI: 10.1103/PhysRevLett.112.221802 PACS numbers: 14.70.Pw, 13.40.Em, 25.30.Rw, 95.35.+d

Introduction.—The completion of the standard model (SM) of particle physics by the discovery of the Higgs particle at the Large Hadron Collider (LHC) is undoubtedly a remarkable success after decades of particle physics experiments [1]. This success, however, also emphasizes one of the major unresolved questions of today's physics: The existence of dark matter in the Universe, which has been meanwhile well established, is one of the most pressing indications of the need for new physics beyond the SM. Because there have yet been no experimental hints from the LHC for supersymmetry, which has for decades provided the most promising candidate for dark matter from particle physics, the search for physics beyond the SM must be extended to more general concepts.

Given the rich structure of the SM, it would not be surprising to have a similar rich structure for a possible "dark sector," consisting of particles and interactions that have only a tiny interaction with SM matter and fields. Most extensions of the SM, e.g., string theory, provide such a rich structure, which has to be broken down to the observed SM.

In recent years, a particularly well-motivated portal to such a dark sector, the search for a massive $U(1)$ gauge boson [2], triggered a vast amount of theoretical and experimental activities. Such a $U(1)$ gauge boson, sometimes called "dark photon" or γ', arises naturally in several extensions of the SM as the lowest-rank interaction of this sector (see, e.g., Refs. [3–5] for an overview).

The residual interaction of a dark photon with SM matter is given in the simplest model by kinematic mixing [6,7], producing an effective interaction $\epsilon e A'_\mu J^\mu$ of the dark-photon field A' with the electric current J. The strength of this interaction is given by the mixing parameter $\epsilon = \sqrt{\alpha'/\alpha}$, equal to the square root of the ratio of dark and SM electromagnetic couplings, which is not required to be small from first principles. Assuming that ϵ vanishes at high energies, ϵ can be generated by perturbative corrections, including particles which are charged both under electromagnetic interaction and the $U(1)$ interaction, leading to a natural scale of $\epsilon \sim 10^{-8} - 10^{-2}$. Including nonperturbative models, values of $\epsilon \sim 10^{-12} - 10^{-3}$ have been discussed [8,9].

In addition to the strong motivation from models and theory, several experimental phenomena could be explained by such a dark photon. A dark sector with an annihilation channel to dark photons could explain, e.g., the positron excess in the Universe measured first by PAMELA [10] and later confirmed by the Fermi LAT Collaboration [11] and AMS-02 [12]. While other positron sources, for example quasars, are also discussed in the literature, the dark-photon annihilation process provides a good fit to the positron spectrum.

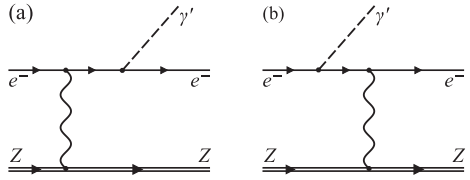

FIG. 1. Radiative production of a γ' in final (a) and initial (b) state on a heavy target nucleus Z. The subsequent decay of the γ' to an electron-positron pair would be the unique signal of such a γ' with a sharp mass distribution.

Of special interest for the parameter range probed in this experiment is the discrepancy of the measured anomalous magnetic moment $(g-2)$ of the muon [13] in comparison with SM calculations [14]. This discrepancy could be explained by loop contributions of dark photons with a mass range of 10–200 MeV/c^2 and a mixing parameter squared around $\epsilon^2 \approx 10^{-5}$ [15,16].

This Letter describes the search for a dark photon in the mass region of 40–300 MeV/c^2 by a fixed-target electron scattering experiment. A possible dark photon could be produced radiatively on a heavy target nucleus with high Z (see Fig. 1), followed by a subsequent decay into an electron-positron pair [17]. Since this decay is suppressed by the small squared mixing parameter ϵ^2, the decay width would be far below the experimental resolution, resulting in a sharp peak in the invariant mass of the produced lepton pair.

This peak is expected to be on top of a smooth background of standard radiative electron-positron pair production via a virtual photon. This background can be calculated in QED; the tools to integrate the background and a possible signal over the acceptance of the experiment were developed and discussed in detail in Refs. [18,19].

Experiment.—The experiment was performed at the spectrometer setup of the A1 Collaboration at the Mainz Microtron (see Ref. [20] for a detailed description). The experimental technique was similar to the technique used in the precursor experiment [21], with a few modifications of the target and of the vacuum system to further reduce multiple scattering and to improve the overall mass resolution.

Table I summarizes the kinematical settings. For all settings, the incoming electron beam of the accelerator hits a target consisting of one or several strips of tantalum foils (99.99% ^{181}Ta); the thickness of each separate foil is between 1 and 6 μm. For each setting, the target configuration was separately optimized for maximum luminosity, with minimized load by radiation background in the focal plane detectors of the spectrometers.

For the detection of the lepton pair from the decay of a possible dark photon, the spectrometers A and B of the A1 setup were placed at their minimal angle (see Table I). With these fixed angles, the settings were adjusted to cover the production of a dark photon in the beam direction and to cover the maximum energy transfer to the dark photon. The choice of the polarity of the spectrometers was given by the background conditions. Since the theoretical description of the background process improved during the analysis, it

TABLE I. Kinematical settings. All settings were centered around the production of lepton pairs in the beam direction and with maximum energy transferred to the pair.

Setting	Central mass (MeV/c^2)	Beam energy E_0 (MeV)	θ_{e+}	p_{e+} (MeV/c)	θ_{e-}	p_{e-} (MeV/c)	e^+ in spectrometer	e^- in spectrometer	Collimator A (msr)	Collimator B (msr)	Target
1	54	180	20.0°	74.0	15.1°	97.1	*A*	*B*	28	5.6	single foil
2	54	180	15.1°	100.3	20.0°	74.0	*B*	*A*	21	5.6	single foil
3	57	180	20.0°	78.7	15.6°	98.0	*A*	*B*	21	5.6	single foil
4	72	240	20.0°	103.6	15.6°	132.0	*A*	*B*	21	5.6	single foil
5	76	255	20.0°	105.0	15.1°	137.3	*A*	*B*	28	5.6	single foil
6	77	255	20.0°	110.1	15.6°	140.4	*A*	*B*	21	5.6	single foil
7	91	300	20.0°	129.5	15.6°	164.6	*A*	*B*	21	5.6	single foil
8	103	345	20.0°	142.0	15.1°	186.5	*A*	*B*	28	5.6	foil stack
9	109	360	20.0°	155.4	15.6°	197.6	*A*	*B*	21	5.6	single foil
10	135	450	20.0°	185.0	15.1°	243.3	*A*	*B*	28	5.6	foil stack
11	138	435	15.6°	244.0	20.0°	190.7	*B*	*A*	21	5.6	single foil
12	138	435	15.6°	233.9	20.0°	190.0	*B*	*A*	21	5.6	single foil
13	138	435	20.0°	190.0	15.6°	244.5	*A*	*B*	21	5.6	single foil
14	138	435	20.0°	190.0	15.6°	234.1	*A*	*B*	21	5.6	single foil
15	150	495	20.0°	213.7	15.6°	271.1	*A*	*B*	21	5.6	foil stack
16	170	570	20.0°	234.0	15.1°	307.3	*A*	*B*	28	5.6	foil stack
17	177	585	20.0°	250.0	15.6°	317.3	*A*	*B*	21	5.6	foil stack
18	202	675	15.1°	367.0	20.0°	277.2	*B*	*A*	21	5.6	single foil
19	218	720	20.0°	309.2	15.6°	392.7	*A*	*B*	21	5.6	foil stack
20	256	855	20.0°	351.0	15.1°	460.3	*A*	*B*	28	5.6	foil stack
21	270	855	15.2°	509.4	22.8°	346.3	*B*	*A*	21	5.6	single foil
22	270	855	15.1°	511.7	20.0°	346.3	*B*	*A*	21	5.6	single foil

turns out that some of these settings were not chosen optimally. The settings of the pilot experiment [21] were included, and were reanalyzed with additional event samples covering the same mass region.

The vacuum system of the spectrometers was connected to the scattering chamber to minimize multiple scattering. Both spectrometers were equipped with four layers of vertical drift chambers for position resolution, two layers of scintillator detectors for trigger and timing purposes, and gas Čerenkov detectors for pion-electron separation and further background reduction.

The beam current of up to $I = 80\ \mu$A was measured with a flux-gate magnetometer (Förster probe). The angular acceptances of the spectrometers were defined by heavy metal collimators. For spectrometer B, a collimator setting of 40 mrad (horizontal) $\times$ 140 mrad (vertical) $= 5.6$ msr was used for all settings, while for spectrometer A two different collimators with 150×140 mrad $= 21$ msr and 200×140 mrad $= 28$ msr were used. The momentum acceptance of the spectrometers was 20% for spectrometer A and 15% for spectrometer B.

Data analysis.—The lepton pair was detected in coincidence between the two spectrometers. For reaction identification, a cut was applied first on a signal in the Čerenkov detectors of both spectrometers with an efficiency of $\approx$98%. The coincidence time between spectrometer A and B was corrected for the path length in spectrometer A of $\approx$10 m and spectrometer B of $\approx$12 m. After this correction, a clear coincidence peak with a width of less than 1 ns (FWHM) was seen. The range of $|\Delta t_{AB}| < 1$ ns was used to identify lepton pairs. The background contribution from random coincidences was estimated by a cut on the sideband with 5 ns $< |\Delta t_{AB}| <$ 15 ns.

Additional cuts were applied for the acceptance of the spectrometers to further reduce the contribution of backscattered particles from the entrance flange of spectrometer B. Finally, cuts on the validity of the overall kinematics were applied to remove, e.g., accidental coincidences where the total energy of the pair exceeds the beam energy.

In total, the background contribution ranges from 4% up to 11% after all cuts. This background contribution is not subtracted for the peak search, but has to be taken into account later in the calculation of the exclusion limit.

For the identified lepton pairs, the invariant pair mass was determined by the four-momenta of the leptons via $m^2_{e+e-} = (p_{e^+} + p_{e^-})^2$. Figure 2 shows the mass distribution of all settings.

To add up the pair mass distribution of all settings, the absolute mass calibration of each setting has to be better than the expected peak width. The magnetic field of the spectrometers was simultaneously monitored with NMR probes to $\delta B/B = 10^{-4}$ and with Hall probes on the $\delta B/B = 5 \times 10^{-4}$ level. This translates, in total, to a mass calibration of better than 100 keV$/c^2$. The calibration was verified at several points by additional measurements of

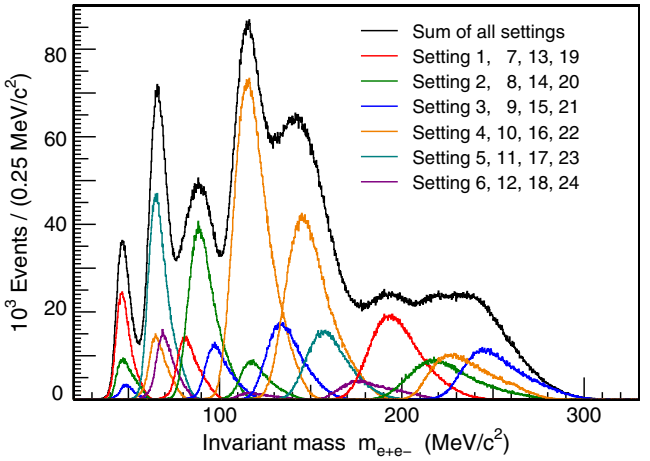

FIG. 2 (color online). Mass distribution of the individual settings (color or shaded) and of the sum (black). The experiment probes the invariant mass region between 40 and 300 MeV$/c^2$.

elastic scattering on tantalum. The position and width of the ^{181}Ta ground state was used to confirm the total calibration and to extract the momentum and angular resolution of the total setup *in situ*. The experimental resolutions were used to tune the detailed simulation of the elastic scattering process to reproduce the elastic peak shape. Finally, the simulation was used to determine the mass resolution and expected dark-photon peak shape, which depend on the mass including radiative corrections. The resulting resolution varies between 210 keV$/c^2$ FWHM, in the lowest mass range, up to 920 keV$/c^2$ FWHM, for the settings of the last experiment.

The estimated peak shape was used to perform a search for a peak in the total mass distribution. For this, the background for each bin was estimated by a local fit of the neighboring bins with a cubic polynomial. The confidence interval was determined using the Feldman-Cousins algorithm [22]. (Please note that in the literature several different approaches were used by different experiments to determine limits for dark-photon searches; however, they differ only by a few percent.) The results were corrected for the leakage of the peak outside the bin. The complete procedure was repeated with shifted binning limits in eight steps.

No significant signal for a dark photon was detected.

Results and interpretation.—Because of the use of thin tantalum foil stacks as targets, the normalization of the cross section contains large uncertainties. However, the identification of the QED background process is very clean, and can be used as normalization. Therefore, to translate the exclusion limit in terms of events to an exclusion limit in terms of the mixing parameter ϵ, we used the ratio of dark-photon production with mixing parameter ϵ divided by the QED background process [17],

$$R = \frac{d\sigma(X \to \gamma' Y \to e^+e^- Y)}{d\sigma(X \to \gamma^* Y \to e^+e^- Y)} = \frac{3\pi}{2N_f}\frac{\epsilon^2}{\alpha}\frac{m_{\gamma'}}{\delta_m}.$$

TABLE II. Systematic uncertainties.

Source	Uncertainty (%)
Calibration of the missing mass determination	0.1
Simulation of the expected peak shape	0.3
Fit of the background shape	0.2
Background subtraction	0.05
Normalization	2
Total (linear sum)	2.7

Here N_f is the ratio of the phase space of the decay into an e^+e^- pair to the phase space of the total decay (equal to 1 below $2m_\mu$), and δ_m is the bin width in mass. Please note that this particular choice of N_f implies that the dark photon decays only into SM matter. Exclusion limits for more general models, with invisible decays into light dark-sector particles with mass $m_X < m_{\gamma'}/2$, can be derived by scaling ϵ^2 with the corresponding branching ratio. For the virtual photon channel we used the background-subtracted mass distribution. To determine the ratio R, both cross sections as calculated in Ref. [18] were integrated over the acceptance of the experiment by standard Monte Carlo methods. Here, the normalization was chosen to reproduce the measured mass distribution.

Please note that in the interpretation of the data in Ref. [21], the cross sections were calculated not including the full antisymmetrization as discussed in Ref. [18]; this leads to an overestimation of the sensitivity by a factor of 2–3. Therefore, these data were included in this analysis and were reanalyzed. Because additional data were taken in the same mass range, roughly the same sensitivity was achieved.

Table II summarizes the systematic uncertainties of the measurement, including the systematic error of the interpretation as a limit in ϵ^2. The contribution of the missing mass calibration was estimated to be 0.1% by varying momentum and angular calibration in the simulation. The quality of the peak shape description via simulation was estimated, by the description of the peak shape of the elastic calibration settings, to contribute less than 2% in the shape itself, leading to an error in the leakage between the bins of 0.3%. The fit of the background by using neighboring bins introduces an additional statistical error from these bins; this is larger than the error in the shape and contributes 0.2% to the systematic error. The subtraction of the background of up to 11% is only used for the normalization and contributes 0.05% to the systematic error. The dominant systematic error originates from the normalization of the total yield, because the mass distribution of the QED calculation differs locally up to 2% from the measured distribution.

Figure 3 shows the resulting 2σ exclusion limits. Also included in the figure are the limits by the APEX [23], WASA-at-COSY [24], KLOE-2 [25], HADES [26], and *BABAR* [27,28] Collaborations. The red line shows the interpretation of the $a_\mu = (g-2)_\mu$ discrepancy as a dark photon with a 2σ error band (dashed lines) and as an exclusion limit (blue shaded region). Also included is the reanalysis of Ref. [29] of the beam dump experiment E774 [30] to extract exclusion limits for dark photons.

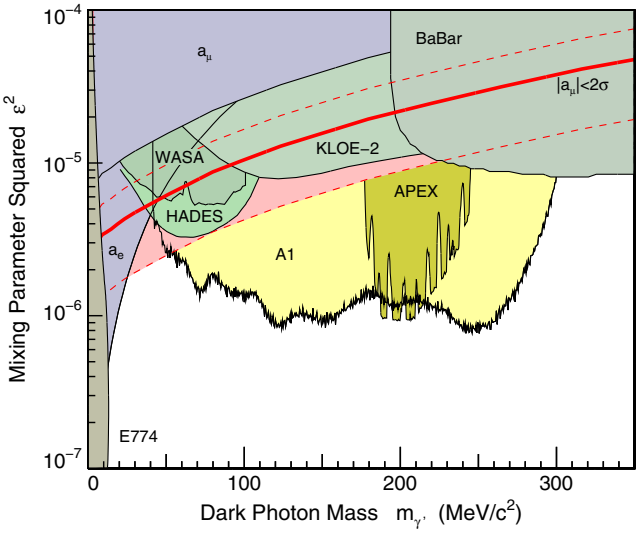

FIG. 3 (color online). Exclusion limits in terms of squared mixing parameter ϵ^2. The yellow (light shaded) area marked with A1 is excluded by this experiment.

With the new measurement presented here, the exclusion limit in the region of the $(g-2)$ anomaly of the muon was improved considerably. While the results of the meson decays by KLOE-2, WASA-at-COSY, and HADES were not able to completely rule out the dark photon as the origin of the anomaly, the new data set clearly covers the possible signal of the anomaly by several sigmas over a large mass range. The remaining undecided mass range of $25\ \mathrm{MeV}/c^2 \lesssim m_{\gamma'} \lesssim 50\ \mathrm{MeV}/c^2$ cannot be covered by the spectrometers of the A1 collaboration without modifications. However, several experiments by different collaborations are already planned to access the low mass region in the near future (see Ref. [19] for a summary).

The authors would like to thank the MAMI accelerator group for the excellent beam quality that made this experiment possible. This work was supported by the Collaborative Research Center 1044 and the State of Rhineland-Palatinate.

*merkel@kph.uni-mainz.de
†Present address: The College of William & Mary, Williamsburg, VA 23185, USA.
‡Present address: MIT-LNS, Cambridge, MA 02139, USA.

[1] S. Chatrchyan *et al.*, Phys. Lett. B **716**, 30 (2012).
[2] P. Fayet, Nucl. Phys. **B347**, 743 (1990).
[3] P. Langacker, Rev. Mod. Phys. **81**, 1199 (2009).
[4] P. Fayet, Phys. Rev. D **81**, 054025 (2010).

[5] J. Beringer *et al.* (Particle Data Group), Phys. Rev. D **86**, 010001 (2012).
[6] B. Holdom, Phys. Lett. **166B**, 196 (1986).
[7] P. Galison and A. Manohar, Phys. Lett. **136B**, 279 (1984).
[8] N. Arkani-Hamed and N. Weiner, J. High Energy Phys. 12 (2008) 104.
[9] R. Essig, P. Schuster, and N. Toro, Phys. Rev. D **80**, 015003 (2009).
[10] O. Adriani *et al.*, Nature (London) **458**, 607 (2009).
[11] M. Ackermann *et al.* (Fermi LAT Collaboration), Phys. Rev. Lett. **108**, 011103 (2012).
[12] M. Aguilar *et al.* (AMS Collaboration), Phys. Rev. Lett. **110**, 141102 (2013).
[13] G. W. Bennett *et al.*, Phys. Rev. D **73**, 072003 (2006).
[14] M. Davier, A. Hoecker, B. Malaescu, and Z. Zhang, Eur. Phys. J. C **71**, 1515 (2011).
[15] P. Fayet, Phys. Rev. D **75**, 115017 (2007).
[16] M. Pospelov, Phys. Rev. D **80**, 095002 (2009).
[17] J. D. Bjorken, R. Essig, P. Schuster, and N. Toro, Phys. Rev. D **80**, 075018 (2009).
[18] T. Beranek, H. Merkel, and M. Vanderhaeghen, Phys. Rev. D **88**, 015032 (2013).
[19] T. Beranek and M. Vanderhaeghen, Phys. Rev. D **89**, 055006 (2014).
[20] K. I. Blomqvist *et al.*, Nucl. Instrum. Methods Phys. Res., Sect. A **403**, 263 (1998).
[21] H. Merkel *et al.* (A1 Collaboration), Phys. Rev. Lett. **106**, 251802 (2011).
[22] G. J. Feldman and R. D. Cousins, Phys. Rev. D **57**, 3873 (1998).
[23] S. Abrahamyan *et al.* (APEX Collaboration), Phys. Rev. Lett. **107**, 191804 (2011).
[24] P. Adlarson *et al.* (WASA-at-COSY Collaboration), Phys. Lett. B **726**, 187 (2013).
[25] D. Babusci *et al.* (KLOE-2 Collaboration), Phys. Lett. B **720**, 111 (2013).
[26] G. Agakishiev *et al.* (HADES Collaboration), Phys. Lett. B **731**, 265 (2014).
[27] B. Aubert *et al.*, Phys. Rev. Lett. **103**, 081803 (2009).
[28] B. Echenard, Adv. High Energy Phys. **2012**, 514014 (2012).
[29] S. Andreas, C. Niebuhr, and A. Ringwald, Phys. Rev. D **86**, 095019 (2012).
[30] A. Bross, M. Crisler, S. Pordes, J. Volk, S. Errede, and J. Wrbanek, Phys. Rev. Lett. **67**, 2942 (1991).